Inorganic Chemistry

Article

pubs.acs.org/IC

Dithiophene-TTF Salts; New Ladder Structures and Spin-Ladder Behavior

Rafaela A. L. Silva,[†] Isabel C. Santos,[†,§] Jonathan Wright,[∥] Joana T. Coutinho,[†] Laura C. J. Pereira,[†] Elsa B. Lopes,[†] Sandra Rabaça,[†] José Vidal-Gancedo,[‡] Concepció Rovira,[‡] Manuel Almeida,[†] and Dulce Belo*[,†]

[†]C2TN, Instituto Superior Técnico, Universidade de Lisboa, Estrada Nacional 10, P-2695-066 Bobadela LRS, Portugal

[‡]Institut de Ciencia de Materials de Barcelona (ICMAB-CSIC) and CIBER-BBN, Campus UAB, E-08193 Bellaterra, Spain

[§]Centro de Química Estrutural, Instituto Superior Técnico, Universidade de Lisboa, P-1049-001 Lisboa, Portugal

[∥]ESRF, The European Synchrotron, 71 Avenue des Martyrs, F-38000 Grenoble, France

Supporting Information

ABSTRACT: (α-DT-TTF)$_2$[Au(i-mnt)$_2$] and (α-DT-TTF)$_2$[Co(mnt)$_2$] are two new salts of the donor α-dithiophene-tetrathiafulvalene with stable diamagnetic anions, both presenting a ladder structure of the donors organized in paired segregated stacks. The first one is isostructural with previously reported closely related compounds and presents a magnetic spin-ladder behavior with $J_{\|}$= 83.5 K and $J_{\perp}$ = 110.3 K as estimated from spin susceptibility data in single crystals. (α-DT-TTF)$_2$[Co(mnt)$_2$] presents a new structural type with a different arrangement of pairs of donor stacks, alternating with stacks of dimerized [Co(mnt)$_2$] anions which are however arranged in an uncorrelated fashion perpendicular to the stacking axis. Due to the strong coupling between the disordered anion chains and the donor chains, this compound does not present a magnetic spin-ladder behavior. The low temperature superstructure of (DT-TTF)$_2$[Cu(mnt)$_2$] below the transition at 235 K, previously known to be associated with a lattice doubling along the stacking axis, was solved by synchrotron radiation diffraction in small single crystals. It is found that this dimerization is due to donor charge localization with the spin carriers being associated with fully oxidized donor species alternating with neutral donors.

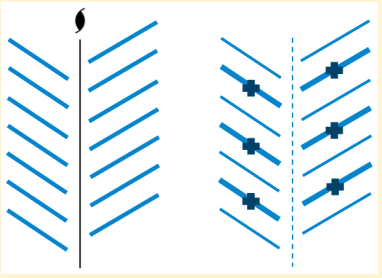

INTRODUCTION

Spin-Ladders are magnetic systems, consisting in a finite number of coupled spin chains and have attracted high interest during the last years due to specific quantum effects. Depending on the number of legs (interacting spin chains), significantly different magnetic behaviors are expected, with a gap in the magnetic excitations for an even number of chains, while the ladders with an odd number of chains are gapless.[1] The interest in these systems has also been stimulated by the exciting prediction that doped ladders can become superconducting due to an effective attraction between holes in chains mediated by magnetic interactions.[1a,b,2]

(DT-TTF)$_2$[Au(mnt)$_2$] (DT-TTF = dithiophenetetrathiafulvalene, mnt = maleonitriledithiolate, Scheme 1) was not only the first organic based molecular spin-ladder system reported,[3] but it also has been at the basis of several related compounds, which so far constitute the largest family of closely related molecular spin ladder systems, whose study offers a possibility to put into evidence important structure−property correlations. In fact, although at present, there are known several molecular spin ladder systems,[4] all of them are based on quite different molecular units and belong to completely different and unrelated structural types with the exception of some compounds derived from (DT-TTF)$_2$[Au(mnt)$_2$], which have been obtained by small molecular modifications, on both the donor and acceptor components.

Indeed similar structures with paired chains and a magnetic spin-ladder behavior have been found in DT-TTF salts with identical diamagnetic anions such as [Cu(mnt)$_2$]$^-$ and [Au(i-mnt)$_2$]$^-$, but these compounds were obtained among several other polymorphs and compounds with different stoichiometries not found in the [Au(mnt)$_2$] salt. The modifications of the donor which can preserve the ladder structure were also found to be rather limited and so far restricted to identical donors ETT-TTF and α-DT-TTF in salts with the [Au(mnt)$_2$] anion (Scheme 1).[5] However, the orientation disorder of the

Scheme 1. Chemical Structures of Electron Donors and Metal Bisdithiolene Anions

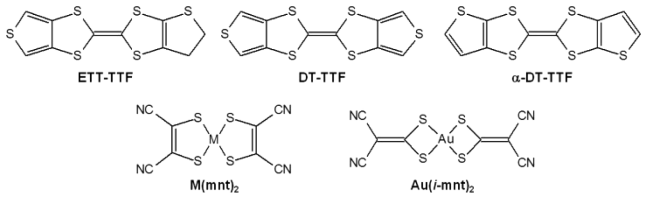

Received: May 6, 2015
Published: July 9, 2015

DOI: 10.1021/acs.inorgchem.5b01013
Inorg. Chem. 2015, 54, 7000−7006

dissymmetric donor ETT-TTF completely destroys the magnetic spin-ladder behavior, because of the large HOMO density in the thiophenic S atom, while in the α-DT-TTF donor, the same type of disorder has much weaker effects due to a negligible contribution of the thiophenic S atom to the HOMO and (α-DT-TTF)$_2$[Au(mnt)$_2$] was found to behave as a weakly disordered spin ladder system.[6]

The emergence of the spin ladder behavior in this family of DT-TTF compounds is known to be associated with a doubling of the cell parameter along the stacking axis upon cooling, which is centered at 220 K, and with a very weak satellite diffraction that is relatively broad in the case of (DT-TTF)$_2$[Au(mnt)$_2$][3] and quite sharp at 235 K in the case of the Cu analogue.[5,7] However, the nature of the spin carrying units in these systems has so far not been clear in spite of IR and Raman spectroscopic investigations[8] and both donor dimerization and charge ordering schemes,[4c,9] as depicted in Figure 1, could explain the observed lattice doubling and the spin-ladder behavior.

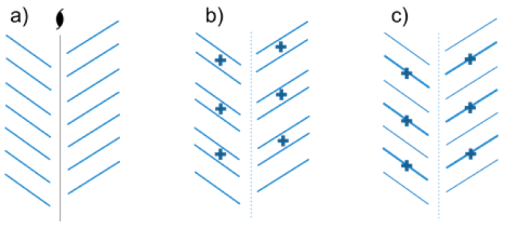

Figure 1. Representation of a pair of donor stacks connected by a screw axis (a) and possible schemes leading to a doubling of the staking axis parameter at low temperatures: bond ordering (b) and charge ordering (c).

It is therefore of obvious interest to explore further salts of α-DT-TTF based on related dithiolene anions and with similar ladder structural arrangement of donors. Previous work has shown that due to the rather low oxidation potential of α-DT-TTF, its salts with [M(mnt)$_2$] anions with M = Ni and Pt have rather different stoichiometries.[6]

In this paper, we describe the new α-DT-TTF salts with electrochemically more stable diamagnetic anions (α-DT-TTF)$_2$[Au(*i*-mnt)$_2$] and (α-DT-TTF)$_2$[Co(mnt)$_2$] and compare their properties with those of the prototype compound (DT-TTF)$_2$[Cu(mnt)$_2$], whose low temperature superstructure could be analyzed in small single crystals using synchrotron radiation. (α-DT-TTF)$_2$[Au(*i*-mnt)$_2$] presents the donors arranged in paired stacks and a spin ladder behavior comparable to (DT-TTF)$_2$[M(mnt)$_2$] with M = Au and Cu. The structure of the Cu salt below 235 K is found to present charge localization with the spin carriers being associated with fully oxidized donor species alternating with neutral donors. (α-DT-TTF)$_2$[Co(mnt)$_2$] presents a new structural type with a different arrangement of pairs of donor stacks, alternating with stacks of dimerized [Co(mnt)$_2$] anions, however without a magnetic spin ladder behavior.

RESULTS AND DISCUSSION

Crystals of (α-DT-TTF)$_2$[Au(*i*-mnt)$_2$] (**1**) and (α-DT-TTF)$_2$[Co(mnt)$_2$] (**2**) were obtained by electrocrystallization of α-DT-TTF in the presence of a tetrabutylammonium salt of the anions in dichloromethane solution, over platinum electrodes and using standard galvanostatic conditions (~1 μA/cm^2) as previously described for similar salts. Single crystals suitable for X-ray diffraction, electron transport, and EPR measurements were collected after about 7 days.

Table 1. Crystal and Refinement Data for (α-DT-TTF)$_2$[Au(*i*-mnt)$_2$] (1), (α-DT-TTF)$_2$[Co(mnt)$_2$] (2), and (DT-TTF)$_2$[Cu(mnt)$_2$] (3)[a]

compound	(α-DT-TTF)$_2$ [Au(*i*-mnt)$_2$] (**1**)	(α-DT-TTF)$_2$ [Co(mnt)$_2$] (**2**)	(DT-TTF)$_2$ [Cu(mnt)$_2$] (**3**)
formula	$C_{28}H_8AuN_4S_{16}$	$C_{28}H_8CoN_4S_{16}$	$C_{28}H_8CuN_4S_{16}$
molec. mass	1110.31	972.27	976.88
T (K)	150(2)	120(2)	120(2)
dimens. (mm)	0.50 × 0.06 × 0.02	0.20 × 0.04 × 0.02	0.40 × 0.10 × 0.08
crystal color	dark brown	dark brown	black
crystal system	monoclinic	triclinic	triclinic
space group	$P2_1/n$	P-1	P-1
a (Å)	17.1678(9)	3.7551 (5)	7.6977(6)
b (Å)	3.8756(2)	15.204(4)	16.6382(12)
c (Å)	26.0522(11)	15.711(3)	26.955(2)
α (deg)	90.00	106.831(7)	78.618(3)
β (deg)	100.208(2)	92.574(4)	89.931(2)
γ (deg)	90.00	96.508(6)	76.638(3)
volume (Å^3)	1705.96(14)	850.2(3)	3513.6(4)
Z	2	1	4
ρ_{calc} (g·cm^{-3})	2.162	1.899	1.973
h, *k*, *l* range	±20, −4/+3, ± 31	±4, ± 18, ± 19	±11, ± 24, ± 39
θ_{max} (deg)	25.03	10.63	12.45
refl. collected	10363	5905	160232
refl. indexed	2972	3065	21422
refl. >2σ (I)	2342	2940	18649
R1	0.0312	0.0829	0.0469
ωR2	0.0618	0.1921	0.1129

[a]Crystallographic data (excluding structure factors) for **2**, **1** and **3** was deposited with the Cambridge Crystallographic Data Centre with nos. CCDC 1062505−7 respectively.

DOI: 10.1021/acs.inorgchem.5b01013
Inorg. Chem. 2015, 54, 7000−7006

(α-DT-TTF)$_2$[Au(i-mnt)$_2$] was analyzed using a conventional X-ray diffractometer and found to crystallize in the monoclinic space group P2$_1$/n being isostructural with the [Au(mnt)$_2$] salts with DT-TTF and α-DT-TTF. Crystal and structural refinement data are listed in Table 1. The asymmetric unit is composed of one α-DT-TTF donor molecule and half [Au(i-mnt)$_2$]$^-$ anion, with the gold atom placed in an inversion center (Figures 2 and 3). Both units are essentially planar. As in the [Au(mnt)$_2$] salt, the donors are disordered, both ends of the molecule presenting the thiophenic sulfur atoms S5 and S8 in two possible positions with occupation factors of 0.70−0.30 and 0.68−0.32, respectively (Figure 2a and Supporting Information, SI, Figure S1).

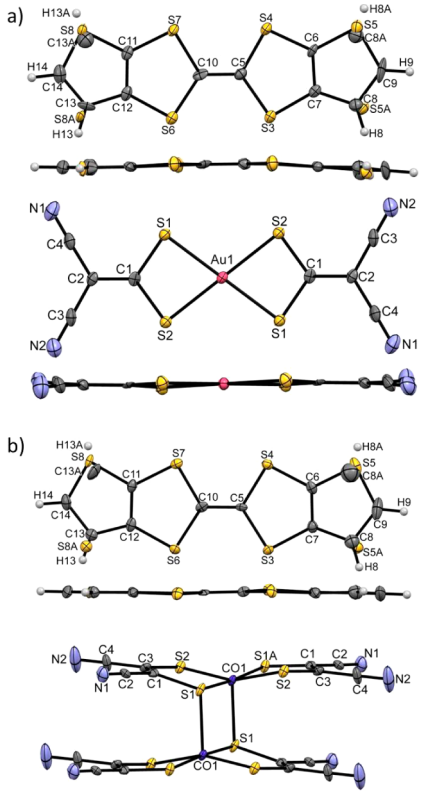

Figure 2. ORTEP views of (α-DT-TTF), [Au(i-mnt)$_2$]$^-$, and [Co(mnt)$_2$]$^-$ units with atom numbering scheme, in the crystal structure of (a) (α-DT-TTF)$_2$[Au(i-mnt)$_2$] (**1**) and (b) (α-DT-TTF)$_2$[Co(mnt)$_2$] (**2**). The [Co(mnt)$_2$]$_2^{2-}$ dimer shown was obtained by the appropriated choice of one position for the Co and S1 atoms.

This disorder results most probably from the orientation disorder of the donors which are obtained primarily in the most stable trans-configuration.[6] As in the previously described (α-DT-TTF)$_2$[Au(mnt)$_2$] salt, this disorder is not expected to have any major consequence in the magnetic properties, in view of the negligible contribution of the thiophenic S atom to the HOMO.[6]

As in the analogous spin-ladder compounds, both donor and acceptor units form segregated stacks along the b-axis, the stacks of the α-DT-TTF donors being arranged in closely connected pairs related by a screw axis (Figure 3).

The donor molecules and the anions are tilted toward the staking axis b by 67.2 and 61.4°, respectively, and the interplanar distances between donor molecules (3.516 Å) are slightly smaller than those found in the [Au(mnt)$_2$] salt (3.557 Å), while those between the Au(i-mnt)$_2$ anions are 3.387 Å. The two donor stacks related by a screw axis are connected by short S···S contacts (S5···S8 and S5···S7) at 3.511 and 3.514 Å, and molecules make a dihedral angle 49.78 Å.

The crystals of (α-DT-TTF)$_2$[Co(mnt)$_2$] suitable for X-ray analysis were of smaller dimensions (0.20 × 0.04 × 0.02 mm^3), and their structure could be solved only by using synchrotron radiation at ID11 at ESRF. The crystal structure is triclinic space group P-1. The asymmetric unit contains one donor molecule and half anion [Co(mnt)$_2$] with the Co atom in two closely spaced positions with 50% occupation near an inversion center, as well as one sulfur atom S1. As in the previous compound, the donor units present a disorder in the thiophenic sulfur atoms S5 and S8 in two possible positions with occupation factors of 0.71−0.39 and 0.43−0.57, respectively (Figure 2b and SI Figure S2).

The donor and acceptor units form segregated stacks along the a-axis. These stacks are arranged in the b,c plane with a packing pattern similar to the previously described structure for **1** and related spin ladder structures, with donor stacks arranged in pairs. However, the donor molecules are not connected by a screw axis and present a different tilting toward the stacking axis a (Figure 3a) with a different overlap mode with a displacement along the donor long axis (Figure 4). The observed disorder in the Co atom position is a consequence of the well-known tendency of Co anions to form dimers [Co(mnt)$_2$]$_2^{2-}$, through axial S—Co bonds, and the observed structure is an average one resulting from the superposition of two possible ways of forming these dimers (Figure 5). The S—Co bond distance 2.38(2) Å is comparable to that of 2.405(3) Å observed in an identical average structure of uncorrelated dimerized chains[10] and 2.493(2) Å in a pyridinum salt with isolated dimers.[11] Each anion column is surrounded by six donor columns, and there are 8 short donor−acceptor contacts (N—S, N—H, S—S) between each anion. The dimerization phase of [Co(mnt)$_2$]$_2^{2-}$ stacks appear however uncorrelated in the b,c plane.

The superstructure of (DT-TTF)$_2$[Cu(mnt)$_2$] below the transition at 235 K could also be determined using synchrotron radiation at ID11 beamline of ESRF in small single crystals obtained as previously described. The superstructure observed at 120 K is associated with rather low intense diffraction peaks corresponding to a doubling of the stacking axis b. While the average structure neglecting these extra peaks corresponds to the typical ladder structure of these compounds as that above-described for **1**, with a monoclinic space group P2$_1$/n, the full structure is now a triclinic space group P-1. The asymmetric unit contains four donor units (A−D) and two anions (E and F). There are now two different donor stacks composed of alternating units A,B and C,D. The four donors present however two distinct geometrical parameters.

The analysis of bond lengths of the donors, especially the central C═C and C—S bonds in the TTF, which are known to be particularly sensitive to the degree of oxidation, clearly show that molecules A and C are fully oxidized, while B and D are neutral (SI Table S7). The intermolecular distances along the staking axis are almost identical. The two anions E and F, although crystallographically distinct, are also identical within experimental uncertainty. Therefore, the doubling of the cell parameter b in the low temperature superstructure is primarily associated with an alternation of neutral and oxidized molecules along the stacking axis, with a charge ordering scheme as

DOI: 10.1021/acs.inorgchem.5b01013
Inorg. Chem. 2015, 54, 7000−7006

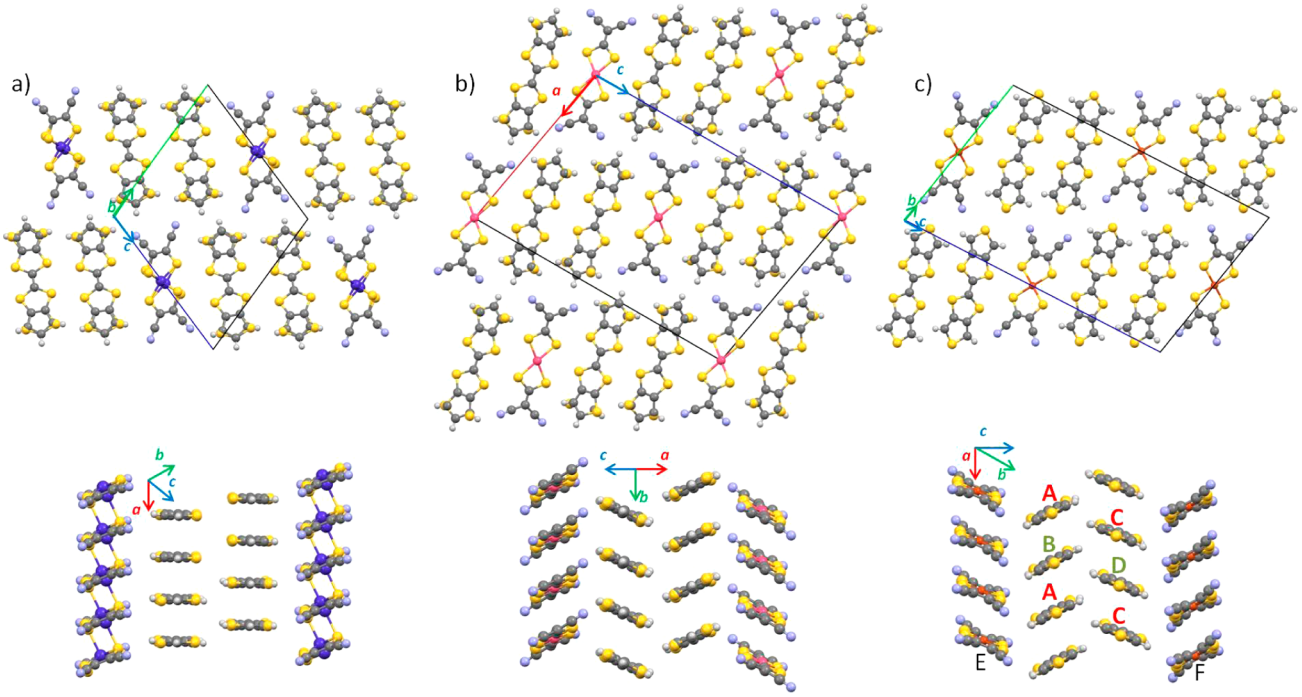

Figure 3. Crystal structure of (a) (α-DT-TTF)$_2$[Co(mnt)$_2$], (b) (α-DT-TTF)$_2$[Au(i-mnt)$_2$], and (c) (DT-TTF)$_2$[Cu(mnt)$_2$]. Top views along the staking axis. Bottom, partial views of layers of neighboring donor and acceptor chains along the molecular chain axis. In (c), the donor molecules A–C are fully oxidized and B–D are neutral.

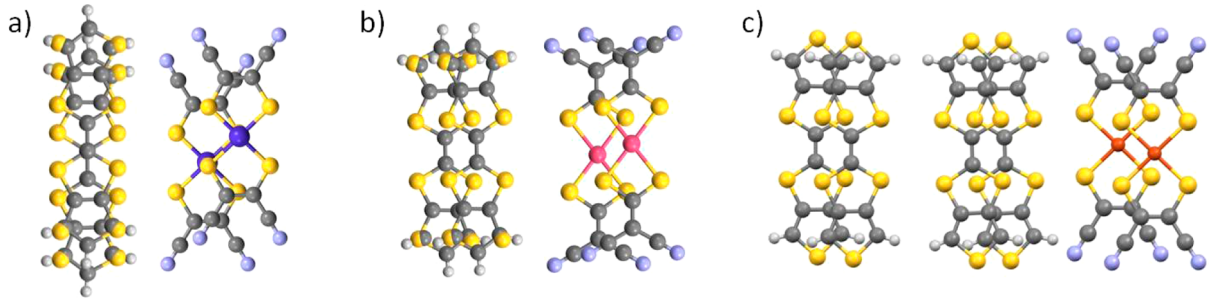

Figure 4. Donor–donor and anion–anion overlap modes in (a) (α-DT-TTF)$_2$[Co(mnt)$_2$], (b) (α-DT-TTF)$_2$[Au(i-mnt)$_2$], and (c) (DT-TTF)$_2$[Cu(mnt)$_2$].

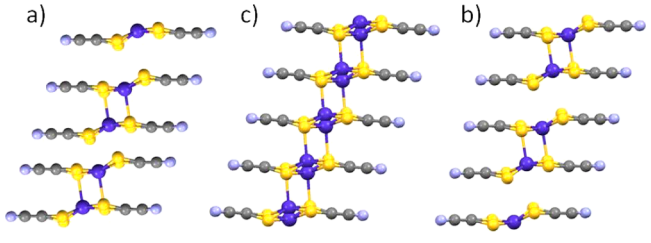

Figure 5. Different dimerization phases of [Co(mnt)$_2$]$_2$ (patterns (a) and (b)) whose overlap leads to the average structure observed (c).

depicted in Figure 1 at right, rather than due to any pairing or bond ordering scheme.

The electrical transport properties of (α-DT-TTF)$_2$[Au(*i*-mnt)$_2$] and (α-DT-TTF)$_2$[Co(mnt)$_2$] were studied by conductivity and thermoelectric power measurements in selected single crystals along their long axis (donor stacking axes *b* and *a* of their respective crystal structures), and the results are shown in Figures 6 and 7 in comparison with those of the related salts of this family. The lattice parameters of these

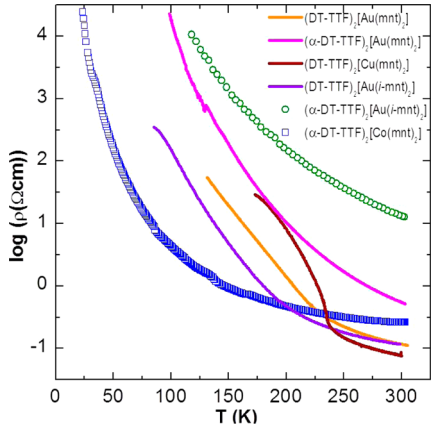

Figure 6. Electrical resistivity of (α-DT-TTF)$_2$[Au(i-mnt)$_2$], (α-DT-TTF)$_2$[Co(mnt)$_2$], and related compounds as a function of temperature.

crystals were in agreement with the described crystal structures, ruling out possible confusion with other phases present in the

DOI: 10.1021/acs.inorgchem.5b01013
Inorg. Chem. 2015, 54, 7000–7006

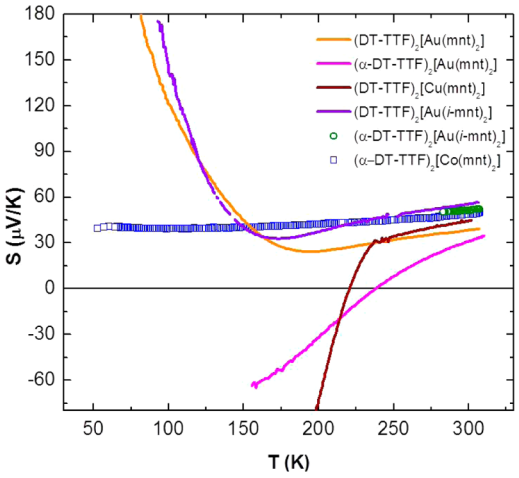

Figure 7. Thermoelectric power of $(\alpha\text{-DT-TTF})_2[Au(i\text{-mnt})_2]$, $(\alpha\text{-DT-TTF})_2[Co(mnt)_2]$, and related compounds as a function of temperature.

preparations. The electrical conductivity of $(\alpha\text{-DT-TTF})_2[Au(i\text{-mnt})_2]$ at room temperature is ~0.1 S/cm, significantly smaller than in $(\alpha\text{-DT-TTF})_2[Au(mnt)_2]$ (2 S/cm)[6] and the related DT-TTF salts (7−40 S/cm),[3b] and with a clear semiconducting regime corresponding to an activation energy of 125 meV (Figure 6). The reduced electrical conductivity of $(\alpha\text{-DT-TTF})_2[Au(i\text{-mnt})_2]$ may reflect smaller intermolecular interactions and or lower crystal quality.

The electrical conductivity of $(\alpha\text{-DT-TTF})_2[Co(mnt)_2]$ at room temperature is much higher than the Au analogue, 7−12 S/cm, with a smaller activation energy and no clear indication of any anomaly, as seen in the spin ladder compounds, which has been associated with charge ordering as more clearly demonstrated in the $(DT\text{-TTF})_2[Cu(mnt)_2]$ with a sharp ordering transition.

Thermoelectric power results in $(\alpha\text{-DT-TTF})_2[Co(mnt)_2]$ with values of 57 μV/K at room temperature, only very slightly decreasing upon cooling to 43 μV/K at 60 K, and with no change of regime that can be associated with charge ordering are consistent with a hopping regime of conduction, possibly between localized states induced by the anion disorder (Figure 7).

The possibility of magnetic measurements in polycrystalline samples using the SQUID technique is restricted by the presence of other phases in electrocrystallization preparations. In fact, the polycrystalline material collected after electrocrystallization presents in the powder X-ray diffraction pattern peaks that do not fit into the structures above-described. The formation of different phases in the same electrocrystallization is not unprecedented in this type of compound since for instance with the anions $[Au(i\text{-mnt})_2]$ and $[Cu(mnt)_2]$ at least two phases where obtained with DT-TTF. Therefore, the magnetic susceptibility analysis of $(\alpha\text{-DT-TTF})_2[Au(i\text{-mnt})_2]$ was restricted to spin susceptibility measurements using EPR in selected single crystals. The selected prismatic crystals have g-factors along the three principal axes (2.0033, 2.0055, and 2.0100) and corresponding line widths ΔHpp (28, 29, and 50G), similar to the related compounds, and are typical of the donor cation-radicals. Upon cooling, the EPR signal intensity, which is proportional to the paramagnetic susceptibility, presents a variation comparable to the previously studied $(\alpha\text{-DT-TTF})_2[Au(mnt)_2]$[6] and $(DT\text{-TTF})_2[M(mnt)_2]$ with M = Au and Cu,[3a,5] as shown in Figure 8. Upon cooling, there is a maximum in the spin susceptibility at ca. 56 K, characteristic of

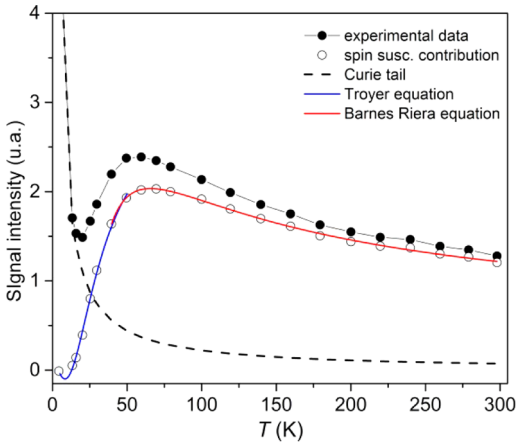

Figure 8. EPR spin susceptibility of $(\alpha\text{-DT-TTF})_2[Au(i\text{-mnt})_2]$ as a function of temperature T. Solid lines correspond to the models of Troyer[12] and Barnes and Riera[13] fits for $T < 50$ K (blue) and 4−300 K (red), respectively. This last model fitting data gives values of $J_\perp$ = 110.3 and $J_\parallel$ = 83.5 K.

a system with localized spins with dominant AFM interactions, followed by a decrease toward zero, which at low temperatures becomes dominated by a Curie tail due to impurities or defects. This behavior is similar to that observed in the above-mentioned closely related spin-ladder compounds.

The spin susceptibility can be considered as the sum of two contributions, that of a ladder system and a Curie Tail (eq 1):

$$\chi = f\chi_{\text{ladder}} + (1 - f)\chi_{\text{Curie}} \quad (1)$$

Following the approach already used in those similar molecular spin-ladder compounds, the spin-ladder contribution could be fitted by a combination of the Troyer and Barnes and Riera equations[12,13] and an energy gap in the spin-excitation spectrum of Δ = 58.3 K was obtained. This fit also allowed the determination of the magnetic interactions between spins along the rails J_{II} and the rungs $J_\perp$ of the ladder as 83.5 and 110.3 K, respectively, which are in good agreement with those obtained for related compounds with the same structure type (Table 2). $(\alpha\text{-DT-TTF})_2[Au(i\text{-mnt})]_2$ is therefore a new example of a weakly disordered spin-ladder comparable to the $[Au(mnt)_2]$ analogue.

The fact that in these spin ladder compounds $J_\perp$ is larger than J_{II} can be understood in view of the low temperature ordering scheme observed in the superstructure of the Cu compound, where ionized molecules sit side by side in nearby stacks and connected by short S···S contacts, but are separated by neutral donors along the stacks.

Table 2. Spin-Ladder Interaction Parameters in Thiophene-TTF Type Compounds

compound	$J_\perp$ (K)	$J_\parallel$ (K)	Δ (K)	ref
$(DT\text{-TTF})_2[Au(mnt)]_2$	142	82	83[a]	3
$(\alpha\text{-DT-TTF})_2[Au(mnt)]_2$	100	54	68	6
$(DT\text{-TTF})_2[Cu(mnt)]_2$[a]	218	121	130	5
$(DT\text{-TTF})_2[Au(i\text{-mnt})]_2$[a]	142	86	82	5
$(\alpha\text{-DT-TTF})_2[Au(i\text{-mnt})]_2$[a]	110	83	58	this work

[a]From single crystal EPR data.

DOI: 10.1021/acs.inorgchem.5b01013
Inorg. Chem. 2015, 54, 7000−7006

The EPR measurements of single crystals of the Co compound did not reveal any spin ladder behavior. The absence of a clear spin-ladder behavior in the Co compound can be understood as a consequence of the random arrangement of the dimerization phase in the anion stacks. Since each anion column has several short contacts with the six nearest donor columns, and the anions chains are uncorrelated in the *b*,*c* plane, it is likely that the random nature of these interactions precludes the required formation of an ordered scheme of charge localization in the donors.

CONCLUSIONS

(α-DT-TTF)$_2$[Au(*i*-mnt)$_2$] is a new example of a weakly disordered spin-ladder magnetic system in this family of closely related compounds. As exemplified by the low temperature structure of (DT-TTF)$_2$[Cu(mnt)$_2$], the spin ladder behavior in this family of compounds is associated with the charge ordering scheme of alternated neutral (diamagnetic) and ionic (paramagnetic) donor units in nearby stacks, explaining why the magnetic interactions along the rails are smaller than along the rungs.

(α-DT-TTF)$_2$[Co(mnt)$_2$] presents a new structural type with a different arrangement of pairs of donor stacks, alternating with stacks of dimerized [Co(mnt)$_2$] anions, however without a magnetic spin ladder behavior due to the stronger disorder effects induced by the anionic chains.

EXPERIMENTAL SECTION

The synthesis of DT-TTF[14] and α-DT-TTF[15] was performed as previously described. The (*n*-Bu$_4$N)[M(mnt)$_2$] (M = Co, Cu) and (*n*-Bu$_4$N)[Au(*i*-mnt)$_2$] salts were also synthesized and purified by recrystallization as previously described.[16,17] Electrocrystallization was achieved in H-shapped two-compartment cells separated by frit glass with Pt electrodes and under galvanostatic conditions. Dichloromethane was also purified using standard procedures and freshly distilled immediately before its use.

Synthesis of (α-DT-TTF)$_2$[Au(i-mnt)$_2$] (1). Crystals were obtained by electrocrystallization from dichloromethane solution of the donor and the acceptor salt, in approximately stoichiometric amounts. The system was sealed under nitrogen and after ~8 days, using a current density of ~1.0 μA.cm^{-2}, the dark brown plate-shaped crystals grown on the anode were collected, washed with dichloromethane, and dried.

Synthesis of (α-DT-TTF)$_2$[Co(mnt)$_2$] (2). Crystals of this salt were obtained by electrocrystallization, at room temperature, from dichloromethane solution of the α-DT-TTF donor and the tetrabutylammonium salt of [Co(mnt)$_2$]$^-$ as electrolyte, in approximately stoichiometric amounts. The system was sealed under nitrogen and after ~10 days, using a current density of ~1 μA/cm^2, the dark brown plate-shaped crystals grown on the anode were collected, washed with dichloromethane, and dried.

Synthesis of (DT-TTF)$_2$[Cu(mnt)$_2$] (3). Black needle shaped crystals, with metallic sheen, were grown by electrocrystallization using the same method already described.[5]

Electrical Transport Properties. Electrical conductivity and thermopower measurements in single crystals were performed in the temperature range of 50−320 K, using a measurement cell attached to the cold stage of a closed cycle helium refrigerator. In the first step, the thermopower was measured using a slow ac (ca. 10−2 Hz) technique,[18] by attaching two 25 μm diameter 99.99% pure Au wires (Goodfellow metals), thermally anchored to two quartz blocks, with Pt paint (Demetron 308A) to the extremities of an elongated sample, as in a previously described apparatus,[19] controlled by a computer.[20] The oscillating thermal gradient was kept below 1 K and was measured with a differential Au-0.05 at. % Fe vs chromel thermocouple of the same type. The absolute thermoelectric power of the sample was obtained after correction for the absolute thermopower of the Au leads, using the data of Huebner.[21]

EPR Measurements. The EPR spectra were obtained using a Bruker ELEXYS E500 X band spectrometer equipped with a field−frequency (*F*/*F*) lock accessory and built in NMR Gaussmeter. A rectangular TE102 cavity was used for the measurements. The signal-to-noise ratio of spectra was increased by accumulation of scans using the *F*/*F* lock accessory to guarantee large field reproducibility. Precautions to avoid undesirable spectral distortions and line broadenings, such as those arising from microwave power saturation and magnetic field over modulation, were also taken into account. To control the temperature in the range from 4 to 300 K an Oxford ESR-900 cryostat was used.

X-ray Diffraction Studies. In the case of (α-DT-TTF)$_2$[Au(*i*-mnt)$_2$], experiments were performed with a Bruker APEX II CCD detector diffractometer using graphite monochromated Mo$K\alpha$ radiation (λ = 0.710 73 Å), in the φ and ω scans mode. A semi-empirical absorption correction was carried out using SADABS.[22] Data collection, cell refinement, and data reduction were done with the SMART and SAINT programs.[23] In the case of (DT-TTF)$_2$[Cu(mnt)$_2$] and (α-DT-TTF)$_2$[Co(mnt)$_2$], single crystal X-ray diffraction was performed on a heavy-duty diffractometer at the Materials Science Beamline ID11 (λ = 0.29520 Å, ESRF, Grenoble, France) using a Frelon2K CCD detector. After conversion of the frame file format, the data were indexed using SMART and integrated with SAINT. They were scaled, combined, and corrected for absorption using SADABS. The structures were solved by direct methods using SIR97[24] and refined by full matrix least-squares methods using the program SHELXL97[25] using the winGX software package.[26] Non-hydrogen atoms were refined with anisotropic thermal parameters, whereas H atoms were placed in idealized positions and allowed to refine while riding on the parent C atom. Molecular graphics were prepared using ORTEP 3.[27]

ASSOCIATED CONTENT

Supporting Information

Figures with details of crystal structure, tables of bond lengths and short contacts in the compounds: (α-DT-TTF)$_2$[Au(*i*-mnt)$_2$], (α-DT-TTF)$_2$[Co(mnt)$_2$], and (DT-TTF)$_2$[Cu(mnt)$_2$]. The Supporting Information is available free of charge on the ACS Publications website at DOI: 10.1021/acs.inorgchem.5b01013.

AUTHOR INFORMATION

Corresponding Author

*E-mail: dbelo@ctn.ist.utl.pt (D.B.).

Notes

The authors declare no competing financial interest.

ACKNOWLEDGMENTS

This work was supported by FCT (Portugal) through contracts PTDC/QUI-QUI/101788/2008 and PTDC/QEQ-SUP/1413/2012 and by DGI, Spain (CTQ2013-40480), the Generalitat de Catalunya (2014SGR0017), the CIBER de Bioingeniera, Biomateriales y Nanomedicina (CIBER-BBN), promoted by ISCIII, Spain, and it also benefited from COST action D35. The authors acknowledge the European Synchrotron Radiation Facility for provision of synchrotron radiation facilities in using beamline ID11. C2TN/IST authors gratefully acknowledge the FCT support through the UID/Multi/04349/2013 project. R.A.L.S. is thankful to FCT for the PhD grant SFRH/BD/86131/2012.

REFERENCES

(1) (a) Dagotto, E.; Rice, T. M. *Science* **1996**, *271*, 618−623. (b) Scalapino, D. J. *Nature* **1995**, *377*, 12−13. (c) Hiroi, Z.; Takano,

DOI: 10.1021/acs.inorgchem.5b01013
Inorg. Chem. 2015, 54, 7000−7006

M. *Nature* **1995**, *337*, 41−43. (d) Azuma, M.; Hiroi, Z.; Tanako, M.; Ishida, K.; Kitaoka, I. *Phys. Rev. Lett.* **1994**, *73*, 3463−3466.
(2) (a) Dagotto, E.; Riera, J.; Scalapino, D. J. *Phys. Rev. B* **1992**, *45*, 5744−5747. (b) Goplan, S.; Rice, T. M.; Sigrist, M. *Phys. Rev. B* **1994**, *49*, 8901−8910. (c) Noack, R. M.; White, S. R.; Scalapino, D. J. *Phys. Rev. Lett.* **1994**, *73*, 882−885. (d) Hayword, C. A.; Poiblanc, D.; Levy, L. P. *Phys. Rev. Lett.* **1995**, *75*, 926−929.
(3) (a) Rovira, C.; Veciana, J.; Ribera, E.; Tarres, J.; Canadell, E.; Rousseau, R.; Mas, M.; Molins, E.; Almeida, M.; Henriques, R. T.; Morgado, J.; Schoeffel, J.-P.; Pouget, J.-P. *Angew. Chem., Int. Ed. Engl.* **1997**, *36*, 2324−2326. (b) Ribera, E.; Rovira, C.; Veciana, J.; Tarrés, J.; Canadell, E.; Rousseau, R.; Molins, E.; Mas, M.; Schoeffel, J.-P.; Pouget, J.-P.; Morgado, J.; Henriques, R. T.; Almeida, M. *Chem.−Eur. J.* **1999**, *5*, 2025−2039. (c) Arcon, D.; Lappas, A.; Margadonna, S.; Prassides, K.; Ribera, E.; Veciana, J.; Rovira, C.; Henriques, R. T.; Almeida, M. *Phys. Rev. B* **1999**, *60*, 4191−4194.
(4) (a) Rovira, C. *Struct. Bonding (Berlin)*; Springer-Verlag: Berlin, Germany, 2001; Vol. *100*, pp 163−188. (b) Fourmigue, M. *Acc. Chem. Res.* **2004**, *37*, 179−186. (c) Clay, R. T.; Mazmudar, S. *Phys. Rev. Lett.* **2005**, *94*, 207206-1−207206-4.
(5) Ribas, X.; Mas-Torrent, M.; Pérez-Benítez, A.; Dias, J. C.; Alves, H.; Lopes, E. B.; Henriques, R. T.; Molins, E.; Santos, I. C.; Wurst, K.; Foury-Leylekian, P.; Almeida, M.; Veciana, J.; Rovira, C. *Adv. Funct. Mater.* **2005**, *15*, 1023−1035.
(6) Silva, R. A. L.; Neves, A. I.; Lopes, E. B.; Santos, I. C.; Coutinho, J. T.; Pereira, L. C. J.; Rovira, C.; Almeida, M.; Belo, D. *Inorg. Chem.* **2013**, 5300−5306.
(7) Dias, J. C.; Lopes, E. B.; Santos, I. C.; Duarte, M. T.; Henriques, R. T.; Almeida, M.; Ribas, X.; Rovira, C.; Veciana, J.; Leylekian, P. F.-; Pouget, J.-P.; Senzier, P. A.-; Jérome, D. *J. Phys. IV France* **2004**, *114*, 497−499.
(8) (a) Wesolowski, R.; Haraldsen, J. T.; Musfeldt, J. L.; Barnes, T.; Torrent, M. M.-; Rovira, C.; Henriques, R. T.; Almeida, M. *Phys. Rev. B* **2003**, *68*, 134405−134413 and erratum; *Phys. Rev. B* **2004**, *70*, 059901. (b) Musfeldt, J. L.; Brown, S.; Mazumdar, S.; Clay, R. T.; Torrent, M. M.-; Rovira, C.; Dias, J. C.; Almeida, M. *Solid State Sci.* **2008**, *10*, 1740−1744.
(9) Yan, Y.; Mazumdar, S.; Ramasesha, S. *Phys. Rev. B* **2006**, *73*, 224418-1−224418-6.
(10) (a) Gama, V.; Henriques, R. T.; Bonfait, G.; Pereira, L. C.; Waerenborgh, J. C.; Santos, I. C.; Duarte, M. T.; Cabral, J. M. P.; Almeida, M. *Inorg. Chem.* **1992**, *31*, 2598−2604. (b) Almeida, M.; Gama, V.; Santos, I. C.; Graf, D.; Brooks, J. S. *CrystEngComm* **2009**, *11*, 1103−1108.
(11) Rodrigues, J. V. *J. Chem. Soc., Dalton Trans.* **1994**, 2655−2660.
(12) (a) Troyer, M.; Tsunetsugu, H.; Würtz, D. *Phys. Rev. B* **1994**, *50*, 13515−13527. (b) Troyer, M.; Zhitomirsky, M. E.; Ueda, K. *Phys. Rev. B* **1997**, *55*, R6117−R6120.
(13) (a) Barnes, T.; Riera, J. *Phys. Rev. B* **1994**, *50*, 6817−6822. (b) Barnes, T.; Dagotto, E.; Riera, J.; Swanson, E. S. *Phys. Rev. B* **1993**, *47*, 3196−3203.
(14) Crivillers, N.; Oxtoby, N. S.; Torrent, M. M-; Veciana, J.; Rovira, C. *Synthesis* **2007**, *10*, 1621−1623.
(15) Silva, R. A. L.; Neves, A. I.; Afonso, M. L.; Santos, I. C.; Lopes, E. B.; Del Pozo, F.; Pfattner, R.; Torrent, M. M.-; Rovira, C.; Almeida, M.; Belo, D. *Eur. J. Inorg. Chem.* **2013**, 2440−2446.
(16) Werden, B. G.; Billig, E.; Gray, H. B. *Inorg. Chem.* **1966**, *5*, 78−81.
(17) (a) Davison, A.; Edelstein, N.; Holm, R. H.; Maki, A. H. *Inorg. Chem.* **1963**, *2*, 1227−1232. (b) Davison, A.; Holm, R. H. *Inorg. Synth.* **1967**, *10*, 8−26.
(18) Chaikin, P. M.; Kwak, J. F. *Rev. Sci. Instrum.* **1975**, *46*, 218−220.
(19) Almeida, M.; Oostra, S.; Alcácer, L. *Phys. Rev. B* **1984**, *30*, 2839−2844.
(20) Lopes, E. B. INETI-Sacavém, internal report, Portugal 1991.
(21) Huebner, R. P. *Phys. Rev. A* **1964**, *135*, A1281−A1921.
(22) Sheldrick, G. M. *SADABS*; Bruker AXS Inc.: Madison, WI, 2004.
(23) *Bruker.SMART and SAINT*; Bruker AXS Inc.: Madison, WI, 2004.
(24) Altomare, A.; Burla, M. C.; Camalli, M.; Cascarano, G.; Giacovazzo, G.; Guagliardi, A.; Moliterni, A. G. G.; Polidori, G.; Spagna, R. *J. Appl. Crystallogr.* **1999**, *32*, 115−119.
(25) Sheldrick, G. M. *SHELXL97, Program for Crystal Structure Refinement*; University of Göttingen: Germany, 1997.
(26) Farrugia, L. J. *J. Appl. Crystallogr.* **1999**, *32*, 837−838.
(27) Farrugia, L. J. *J. Appl. Crystallogr.* **1997**, *30*, 565.

DOI: 10.1021/acs.inorgchem.5b01013
Inorg. Chem. 2015, 54, 7000−7006